Supplement of Atmos. Chem. Phys., 23, 10325–10347, 2023
https://doi.org/10.5194/acp-23-10325-2023-supplement

Atmospheric Chemistry and Physics
Open Access

Supplement of

Source apportionment study on particulate air pollution in two high-altitude Bolivian cities: La Paz and El Alto

Valeria Mardoñ

Correspondence to: Valeria Mardoñez (valeria.mardonez@univ-grenoble-alpes.fr)

Table S1. Bolivian air quality guidelines[1]

Pollutant	***Concentration***	***Period/ statistic characterization***
Carbon Monoxide (CO)	10 mg m^{-3}	8h mean
	40 mg m^{-3}	1h mean
Sulfur dioxide (SO_2)	80 µg m^{-3}	annual mean
	365 µg m^{-3}	24h mean
Nitrogen dioxide (NO_2)	150 µg m^{-3}	24h mean
	400 µg m^{-3}	1h mean
Total suspended particles (TSP)	260 µg m^{-3}	24h mean
	75 µg m^{-3}	annual mean
Particles smaller than 10 µm (PM_{10})	150 µg m^{-3}	24h mean
	50 µg m^{-3}	annual mean
Ozone (O3)	236 µg m^{-3}	1h mean
Lead (Pb)	1.5 µg m^{-3}	3-month mean

Figure S1. Photographs taken at the sampling sites (Left: El Alto sampling site; right: La Paz sampling site)

[1] The concentration values are referred to normal concentrations of pressure and temperature ($\overline{T} = 298\ K$, $\overline{P} = 1013.5\ hPa$)

Figure S2. Sampling sites. ©OpenStreetMap contributors 2020. Distributed under a Creative Commons BY-SA License

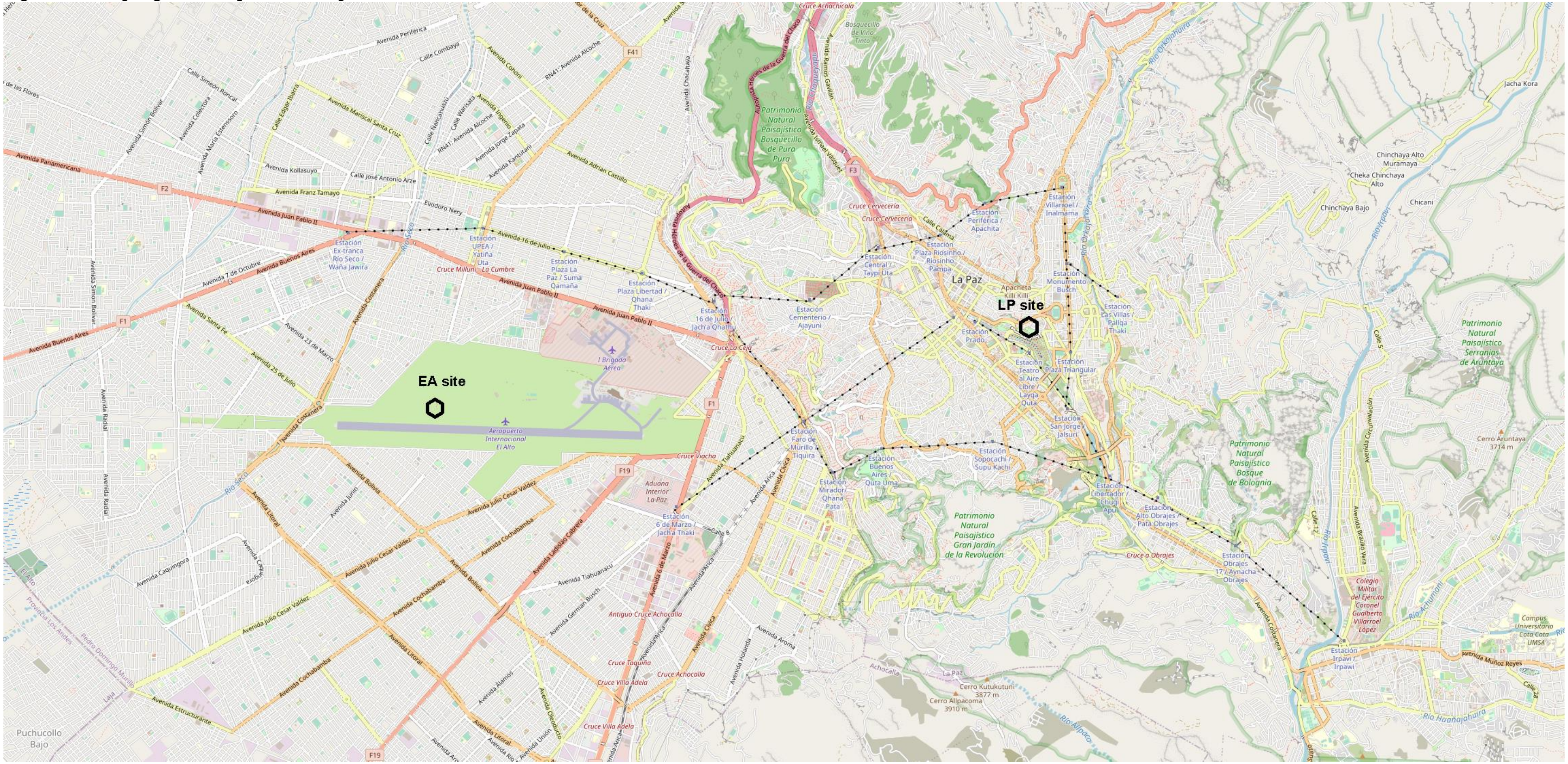

Table S2. Mean, median and standard deviation (sd) of the measured ambient concentrations (above the mean QL, after excluding outliers and samples collected during festivities or the day after, e.g. San Juan, Christmas and New Year). For STP concentrations, ambient concentrations in El Alto must be multiplied by a factor 1.52 and 1.46 for La Paz.

					El Alto (EA)				La Paz (LP)			
Group	**Specie**	**Analysis**	**Units**	**mean QL**	**mean**	**median**	**sd**	**n**	**mean**	**median**	**sd**	**n**
	particulate matter (PM)	gravimetry	[μg m^{-3}]	---	29.9	28.9	12.0	93	27.18	27.07	8.91	103
carbonaceous aerosols	**organic carbon (OC)**	thermal-optical analysis (Cavalli et al., 2010)	[μg m^{-3}]	0.21	3.51	3.48	1.57	93	3.85	3.68	1.78	103
	elemental carbon (EC)		[μg m^{-3}]	0.02	1.46	1.41	0.60	93	1.59	1.57	0.78	103
polyhydric alcohols	**arabitol**	high performance liquid chromatography (HPLC)	[ng m^{-3}]	0.77	2.09	1.79	1.08	83	3.75	3.18	2.28	100
	sorbitol		[ng m^{-3}]	0.79	9.13	5.34	10.77	75	13.88	7.75	17.38	87
	mannitol		[ng m^{-3}]	0.77	3.82	3.37	2.67	88	6.73	5.30	4.53	97
monosaccharide anhydrides	**levoglucosan**		[ng m^{-3}]	0.62	87.73	66.47	76.80	93	79.00	46.26	83.15	101
	mannosan		[ng m^{-3}]	0.77	7.52	4.32	9.02	89	7.46	3.33	10.08	98
	galactosan	(Piot et al., 2012)	[ng m^{-3}]	0.31	3.91	1.65	5.74	91	4.31	1.86	6.09	95
saccharides	**glucose**		[ng m^{-3}]	0.77	14.35	13.81	5.84	93	22.07	22.33	8.81	102
ions	**methanesulfonic acid (MSA^-)**	ionic chromatography (IC)	[ng m^{-3}]	0.06	3.93	3.57	1.87	93	4.38	4.05	2.48	88
	chloride (Cl^-)		[ng m^{-3}]	5.56	217.51	152.27	235.80	93	65.24	52.56	52.79	102
	nitrate (NO_3^-)		[ng m^{-3}]	11.02	609.72	551.21	359.84	92	555.16	482.23	321.65	102
	sulfate (SO_4^{2-})		[ng m^{-3}]	5.29	1247.06	1068.66	723.87	93	1252.77	1098.03	769.54	102
	oxalate (Ox^-)	(Jaffrezo et al., 2005)	[ng m^{-3}]	1.64	50.07	45.75	43.71	73	44.95	24.11	58.18	91
	sodium (Na^+)		[ng m^{-3}]	10.47	52.05	46.35	32.64	86	40.94	39.59	21.10	95
	ammonium (NH_4^+)		[ng m^{-3}]	8.74	511.29	451.65	399.06	93	403.81	333.12	308.04	102
	potassium (K^+)		[ng m^{-3}]	2.76	77.41	68.44	52.61	93	73.34	56.82	55.77	102
	magnesium (Mg^+)		[ng m^{-3}]	0.62	25.14	22.72	12.72	93	24.33	22.45	12.77	102
	calcium (Ca^+)		[ng m^{-3}]	3.53	362.51	312.20	201.63	93	256.30	222.58	136.51	102
metals	**aluminum (Al)**	inductively coupled plasma atomic emission spectrometry (ICP-AES)	[μg m^{-3}]	0.003	1.681	1.582	0.928	93	1.133	1.035	0.563	101
	calcium (Ca)		[μg m^{-3}]	0.001	0.428	0.386	0.218	93	0.350	0.328	0.181	101
	potassium (K)		[μg m^{-3}]	0.001	0.529	0.527	0.287	93	0.394	0.361	0.196	101
	sodium (Na)		[μg m^{-3}]	0.001	0.137	0.135	0.078	93	0.110	0.106	0.060	101
	magnesium (Mg)		[μg m^{-3}]	0.001	0.160	0.156	0.083	93	0.125	0.125	0.059	101
	iron (Fe)		[μg m^{-3}]	0.001	0.932	0.900	0.501	93	0.669	0.590	0.357	101
	lithium (Li)	inductively coupled plasma mass	[ng m^{-3}]	0.05	1.60	1.42	0.96	93	1.04	0.92	0.57	101
	beryllium (Be)		[ng m^{-3}]	0.05	0.10	0.10	0.02	49	0.08	0.08	0.02	27
	phosphor (P)		[ng m^{-3}]	0.05	37.08	34.43	17.91	93	25.48	22.66	11.94	101

	scandium (Sc)	spectrometry (ICP-MS)	[ng m^{-3}]	0.05	0.24	0.21	0.13	35	0.20	0.20	0.09	25
	titanium (Ti)		[ng m^{-3}]	0.05	80.15	74.41	44.71	93	55.83	50.55	27.76	101
	vanadium (V)		[ng m^{-3}]	0.05	2.04	2.01	1.08	88	1.54	1.49	0.73	97
	chromium (Cr)	(Querol et al., 2001)	[ng m^{-3}]	0.05	2.66	1.84	4.52	78	2.36	2.02	1.45	97
	manganese (Mn)		[ng m^{-3}]	0.05	16.48	15.75	8.71	93	12.69	11.90	6.19	101
	cobalt (Co)		[ng m^{-3}]	0.05	0.36	0.32	0.18	91	0.24	0.22	0.11	99
	nickel (Ni)		[ng m^{-3}]	0.05	1.18	0.96	1.29	83	1.12	0.86	0.84	99
	cupper (Cu)		[ng m^{-3}]	0.05	2.89	2.51	1.89	90	4.25	3.91	2.52	101
	zinc (Zn)		[ng m^{-3}]	0.05	12.72	12.63	5.51	93	11.68	11.24	5.47	100
	gallium (Ga)		[ng m^{-3}]	0.05	0.40	0.39	0.23	90	0.29	0.26	0.15	101
	germanium (Ge)		[ng m^{-3}]	0.05	0.11	0.11	0.04	21	0.13	0.11	0.07	8
	arsenic (As)		[ng m^{-3}]	0.05	1.81	1.53	1.07	93	1.03	0.98	0.46	101
	selenium (Se)		[ng m^{-3}]	0.05	0.09	0.10	0.02	16	0.10	0.09	0.03	17
	rubidium (Rb)		[ng m^{-3}]	0.05	3.12	2.88	1.76	93	2.11	1.88	1.10	101
	strontium (Sr)		[ng m^{-3}]	0.05	3.45	3.36	1.90	93	2.64	2.42	1.33	101
	yttrium (Y)		[ng m^{-3}]	0.05	0.43	0.42	0.23	83	0.37	0.31	0.26	85
	zirconium (Zr)		[ng m^{-3}]	0.40	7.49	7.63	1.88	93	6.25	5.99	1.86	100
	niobium (Nb)		[ng m^{-3}]	0.05	0.30	0.29	0.13	93	0.23	0.23	0.09	101
	molibdene (Mo)		[ng m^{-3}]	0.05	1.21	1.09	0.74	49	1.39	1.00	1.13	29
	cadmium (Cd)		[ng m^{-3}]	0.05	0.14	0.13	0.06	90	0.09	0.08	0.02	57
	tin (Sn)		[ng m^{-3}]	0.05	0.58	0.44	0.43	92	0.40	0.36	0.22	101
	antimony (Sb)		[ng m^{-3}]	0.05	1.05	0.80	0.83	91	0.95	0.78	0.67	101
	cesium (Cs)		[ng m^{-3}]	0.05	0.34	0.29	0.19	90	0.22	0.21	0.12	97
	barium (Ba)		[ng m^{-3}]	0.05	14.60	14.48	7.24	90	15.64	15.58	7.46	101
	lanthanum (La)		[ng m^{-3}]	0.05	0.82	0.81	0.42	92	0.58	0.54	0.27	101
	cerium (Ce)		[ng m^{-3}]	0.05	1.65	1.62	0.90	93	1.22	1.16	0.67	101
	praseodymium (Pr)		[ng m^{-3}]	0.05	0.20	0.20	0.10	86	0.17	0.17	0.06	94
	neodymium (Nd)		[ng m^{-3}]	0.05	0.75	0.73	0.41	92	0.52	0.49	0.25	101
	samarium (Sm)		[ng m^{-3}]	0.05	0.15	0.15	0.07	79	0.11	0.12	0.04	73
	europium (Eu)		[ng m^{-3}]	0.05	0.07	0.07	0.01	26	0.07	0.07		1
	gadolinium (Gd)		[ng m^{-3}]	0.05	0.14	0.14	0.06	73	0.11	0.10	0.05	73
	terbium (Tb)		[ng m^{-3}]	0.05	0.07	0.07	0.01	46	0.07	0.07	0.01	18
	dysprosium (Dy)		[ng m^{-3}]	0.05	0.12	0.11	0.04	61	0.10	0.08	0.05	59
	holmium (Ho)		[ng m^{-3}]	0.05	0.07	0.07	0.01	47	0.07	0.07	0.00	6

	erbium (Er)		[ng m^{-3}]	0.05	0.07	0.07	0.01	35	0.07	0.07	0.01	34
	thulium (Tm)		[ng m^{-3}]	0.05				0				0
	ytterbium (Yb)		[ng m^{-3}]	0.05	0.07	0.07	0.01	34	0.07	0.07	0.02	57
	lutetium (Lu)		[ng m^{-3}]	0.05				0				0
	hafnium (Hf)		[ng m^{-3}]	0.40	0.40	0.40		1	0.42	0.41	0.01	9
	tantalum (Ta)		[ng m^{-3}]	0.05				0				0
	tungsten (W)		[ng m^{-3}]	0.05	0.24	0.16	0.23	84	0.20	0.13	0.15	81
	thallium (Tl)		[ng m^{-3}]	0.05	0.07	0.07	0.01	2				0
	lead (Pb)		[ng m^{-3}]	0.05	2.87	2.52	1.61	93	2.05	1.84	1.17	100
	bismuth (Bi)		[ng m^{-3}]	0.05	0.26	0.12	0.46	29	0.19	0.12	0.19	19
	thorium (Th)		[ng m^{-3}]	0.05	0.40	0.34	0.28	89	0.26	0.22	0.18	97
	uranium (U)		[ng m^{-3}]	0.05	0.09	0.09	0.03	48	0.10	0.08	0.06	36
polyaromatic hydrocarbons (PAH)	**phenanthrene (Phe)**	high performance liquid chromatography (HPLC- Fluo) (Besombes et al., 2001)	[ng m^{-3}]	0.008	0.036	0.032	0.021	88	0.045	0.040	0.025	100
	anthracene (An)		[ng m^{-3}]	0.001	0.004	0.003	0.002	90	0.005	0.004	0.003	99
	fluoranthene (Fla)		[ng m^{-3}]	0.002	0.102	0.069	0.097	90	0.083	0.052	0.086	102
	pyrene (Pyr)		[ng m^{-3}]	0.003	0.123	0.082	0.119	91	0.105	0.070	0.107	102
	triphenylene (Tri)		[ng m^{-3}]	0.002	0.080	0.063	0.070	91	0.052	0.036	0.052	101
	retene (Ret)		[ng m^{-3}]	0.000	0.103	0.039	0.152	87	0.045	0.019	0.054	91
	benzo(a)anthracene (BaA)		[ng m^{-3}]	0.008	0.196	0.132	0.171	90	0.147	0.092	0.152	97
	chrysene (Chr)		[ng m^{-3}]	0.004	0.235	0.200	0.182	91	0.165	0.115	0.165	102
	benzo(e)pyrene (BeP)		[ng m^{-3}]	0.005	0.273	0.215	0.282	91	0.228	0.170	0.235	102
	benzo(b)fluoranthene (BbF)		[ng m^{-3}]	0.005	0.250	0.221	0.164	90	0.202	0.165	0.162	102
	benzo(k)fluoranthene (BkF)		[ng m^{-3}]	0.002	0.104	0.096	0.070	90	0.081	0.063	0.067	100
	benzo(a)pyrene (BaP)		[ng m^{-3}]	0.002	0.122	0.094	0.108	90	0.124	0.085	0.116	101
	benzo(g,h,i)perylene (BghiP)		[ng m^{-3}]	0.008	0.410	0.387	0.228	90	0.404	0.351	0.291	101
	dibenzo(a,h)anthracene (DBahA)		[ng m^{-3}]	0.000	0.010	0.006	0.010	88	0.008	0.005	0.009	101
	indeno(1,2,3-cd)pyrene (IP)		[ng m^{-3}]	0.005	0.218	0.214	0.136	91	0.196	0.155	0.144	102
	coronene (Cor)		[ng m^{-3}]	0.002	0.251	0.237	0.143	91	0.268	0.216	0.190	100
alkanes	**C11**	gas chromatography–mass spectrometry (GS-MS)	[ng m^{-3}]	0.070	0.698	0.712	0.358	16	0.559	0.455	0.431	20
	C12		[ng m^{-3}]	0.170	0.254	0.254	0.052	4	1.588	0.865	1.846	3
	C13		[ng m^{-3}]	0.115	0.217	0.184	0.095	19	0.284	0.231	0.244	14
	C14		[ng m^{-3}]	0.070	0.126	0.107	0.036	7	0.121	0.108	0.024	3
	C15		[ng m^{-3}]	0.070	0.381	0.103	0.686	6	0.253	0.124	0.385	12
	C16		[ng m^{-3}]	0.115	0.194	0.170	0.049	3	0.224	0.176	0.119	6

	C17	(Golly, 2014)	[ng m^{-3}]	0.138	0.228	0.219	0.061	33	0.236	0.229	0.058	20
	C18		[ng m^{-3}]	0.128	0.279	0.273	0.117	47	0.292	0.273	0.198	39
	C19		[ng m^{-3}]	0.109	0.571	0.548	0.404	62	0.449	0.376	0.271	55
	C20		[ng m^{-3}]	0.110	1.302	1.093	1.106	71	0.908	0.718	0.783	74
	C21		[ng m^{-3}]	0.339	2.375	1.691	2.056	75	1.674	0.923	1.611	93
	C22		[ng m^{-3}]	0.186	3.118	2.595	2.762	87	2.060	1.128	2.139	101
	C23		[ng m^{-3}]	0.314	3.149	2.634	2.552	86	2.482	1.398	2.443	100
	C24		[ng m^{-3}]	0.231	2.760	2.240	2.157	89	2.278	1.414	2.168	100
	C25		[ng m^{-3}]	0.598	2.849	2.265	1.889	83	2.500	1.692	1.991	97
	C26		[ng m^{-3}]	0.175	2.229	1.917	1.394	90	2.091	1.479	1.627	101
	C27		[ng m^{-3}]	0.580	2.678	2.148	1.847	84	2.714	1.982	2.255	100
	C28		[ng m^{-3}]	0.292	1.719	1.555	1.049	88	1.725	1.251	1.320	100
	C29		[ng m^{-3}]	0.841	2.891	2.306	2.015	83	2.920	1.861	3.077	93
	C30		[ng m^{-3}]	0.288	1.254	1.048	0.810	86	1.205	0.846	0.967	95
	C31		[ng m^{-3}]	0.570	2.348	1.647	1.785	82	2.300	1.429	2.464	83
	C32		[ng m^{-3}]	0.070	0.807	0.652	0.584	84	0.747	0.540	0.669	97
	C33		[ng m^{-3}]	0.070	0.755	0.658	0.538	84	0.825	0.577	0.830	89
	C34		[ng m^{-3}]	0.070	0.564	0.429	0.423	73	0.480	0.359	0.392	82
	C35		[ng m^{-3}]	0.070	0.629	0.429	0.556	68	0.484	0.293	0.474	77
	C36		[ng m^{-3}]	0.070	0.381	0.249	0.358	53	0.357	0.271	0.321	52
	C37		[ng m^{-3}]	0.070	0.394	0.255	0.468	36	0.198	0.166	0.151	24
	C38		[ng m^{-3}]	0.070	0.281	0.187	0.258	15	0.175	0.128	0.126	18
	C39		[ng m^{-3}]	0.070	0.351	0.224	0.362	17	0.164	0.114	0.122	24
	C40		[ng m^{-3}]	0.070	0.319	0.259	0.231	12	0.106	0.100	0.025	9
	Pristane		[ng m^{-3}]	0.070	0.189	0.147	0.164	25	0.258	0.163	0.204	24
	Phytane		[ng m^{-3}]	0.070	0.180	0.161	0.082	23	0.196	0.150	0.139	36
Methyl PAH	**2-methyl-naphthalene**		[ng m^{-3}]	0.019				0				0
	1-methyl-fluorene		[ng m^{-3}]	0.007				0	0.040	0.011	0.051	3
	3-methyl-phenanthrene		[ng m^{-3}]	0.025				0	0.125	0.125	0.141	2
	2-methyl-phenanthrene		[ng m^{-3}]	0.014				0	0.018	0.017	0.005	7
	2-methyl-anthracene		[ng m^{-3}]	0.014				0	0.041	0.041	0.035	2
	4/9-methyl-phenanthrene		[ng m^{-3}]	0.014				0	0.040	0.040		1
	1-methyl-phenanthrene		[ng m^{-3}]	0.007	0.010	0.010		1	0.022	0.013	0.029	9
	4-methyl-pyrene		[ng m^{-3}]	0.007	0.019	0.015	0.012	25	0.022	0.015	0.015	32

	1-methyl-pyrene		[ng m^{-3}]	0.007	0.024	0.017	0.016	27	0.025	0.017	0.018	37
	1+3-Methyl-fluorene		[ng m^{-3}]	0.007	0.016	0.015	0.005	13	0.017	0.014	0.006	14
	Methyl-fluorene/pyrene		[ng m^{-3}]	0.007	0.015	0.011	0.008	20	0.016	0.016	0.007	21
	1-methylfluoranthene		[ng m^{-3}]	0.007	0.017	0.015	0.009	21	0.020	0.014	0.013	26
	3-methyl-chrysene		[ng m^{-3}]	0.008	0.034	0.031	0.022	32	0.039	0.026	0.037	54
	Methyl-chrysene/BenzoAnthracene		[ng m^{-3}]	0.007	0.016	0.014	0.008	28	0.022	0.016	0.016	39
thiophens	**DBT (DiBenzoThiophen)**		[ng m^{-3}]	0.007	0.011	0.011	0.003	4	0.024	0.013	0.022	7
	PheT(4,5) (Phenanthro(4,5 bcd)Thiophen)		[ng m^{-3}]	0.007	0.012	0.011	0.004	4	0.016	0.011	0.016	16
	BNT(2,1) (Benzo(b)Naphto(2,1 d)Thiophen)		[ng m^{-3}]	0.027	0.027	0.027	0.006	7	0.040	0.039	0.020	14
	BNT(1,2) (Benzo(b)Naphto(1,2 d)Thiophen)		[ng m^{-3}]	0.007	0.009	0.010	0.001	3	0.016	0.010	0.009	9
	BNT(2,3) (Benzo(b)Naphto(2,3 d)Thiophen)		[ng m^{-3}]	0.007	0.010	0.010	0.002	12	0.017	0.015	0.009	12
	DNT(2,1) (Dinaphto (2,1) Thiophen)		[ng m^{-3}]	0.007	0.014	0.011	0.008	3	0.014	0.012	0.006	3
	BPT(2,1) (Benzo(b)Phenanto(2,1d)thiophen)		[ng m^{-3}]	0.007				0				0
hopanes	**HP1 (Trisnorneohopane)**		[ng m^{-3}]	0.012	0.060	0.041	0.048	46	0.074	0.049	0.065	64
	HP2 (17α(H)-Trisnorhopane)		[ng m^{-3}]	0.013	0.047	0.038	0.031	54	0.056	0.039	0.044	94
	HP3 (17α(H)-21β(H)-Norhopane)		[ng m^{-3}]	0.007	0.143	0.097	0.122	87	0.215	0.147	0.183	99
	HP4 (17α(H)-21β(H)-Hopane)		[ng m^{-3}]	0.011	0.179	0.119	0.150	83	0.255	0.168	0.212	99
	HP5 (17α(H)-21β(H)-22S-Homohopane)		[ng m^{-3}]	0.007	0.077	0.050	0.064	77	0.109	0.069	0.093	98
	HP6 (17α(H)-21β(H)-22R-Homohopane)		[ng m^{-3}]	0.007	0.059	0.035	0.053	72	0.081	0.050	0.074	99
	HP7 (17α(H)-21β(H)-22S-Bishomohopane)		[ng m^{-3}]	0.007	0.057	0.036	0.053	73	0.077	0.043	0.072	100
	HP8 (17α(H)-21β(H)-22R-Bishomohopane)		[ng m^{-3}]	0.007	0.042	0.026	0.034	66	0.058	0.037	0.051	94
	HP9 (17α(H)-21β(H)-22S-Trishomohopane)		[ng m^{-3}]	0.007	0.044	0.023	0.043	68	0.057	0.031	0.055	89
	HP10 (17α(H)-21β(H)-22R-Trishomohopane)		[ng m^{-3}]	0.007	0.038	0.024	0.028	57	0.043	0.024	0.039	77
	DMPT (6,10,14-trimethyl-2-pentadecanone)		[ng m^{-3}]	0.055	0.749	0.524	0.637	89	0.984	0.631	1.345	102
methoxyphenols	**Vanillin**		[ng m^{-3}]	0.017	0.199	0.162	0.119	22	0.172	0.144	0.101	22
	Acetovanillone		[ng m^{-3}]	0.055	0.280	0.236	0.169	27	0.272	0.095	0.520	16
	Guaiacyl acetone		[ng m^{-3}]	0.057	0.239	0.226	0.117	15	0.161	0.143	0.086	14
	Coniferylaldehyde		[ng m^{-3}]	0.056	0.260	0.224	0.137	4	0.352	0.281	0.199	4

	Vanillic acid		[ng m^{-3}]	0.018	0.577	0.423	0.449	46	0.713	0.533	0.723	40
	Homovanillic acid		[ng m^{-3}]	0.014	0.218	0.175	0.079	3	0.087	0.087	0.034	2
	Syringol		[ng m^{-3}]	0.006				0	0.066	0.066		1
	4-methylsyringol		[ng m^{-3}]	0.006				0	0.032	0.032		1
	4-propenylsyringol		[ng m^{-3}]	0.028				0	0.093	0.093		1
	Acetosyringone		[ng m^{-3}]	0.028	0.398	0.353	0.227	33	0.420	0.409	0.220	31
	Syringyl acetone		[ng m^{-3}]	0.017	0.181	0.181		1	0.089	0.089		1
	Sinapyl aldehyde		[ng m^{-3}]	0.056	0.160	0.160		1	0.348	0.348	0.204	2
	Syringic acid		[ng m^{-3}]	0.018	0.322	0.283	0.182	34	0.442	0.331	0.328	33
sterols	**Cholesterol**		[ng m^{-3}]	0.056	2.300	1.926	1.412	11	1.534	1.413	0.858	22
methyl-nitricatechols	**3methylcatechol**		[ng m^{-3}]	0.070				0	0.133	0.133		1
	4-methylcatechol		[ng m^{-3}]	0.084				0				0
	4nitroguaiacol		[ng m^{-3}]	0.300	0.414	0.414		1				0
	4nitrocatechol		[ng m^{-3}]	0.140	1.001	0.806	0.601	14	1.602	1.458	1.130	22
	3-methyl-6-nitrocatechol		[ng m^{-3}]	0.124				0				0
	4-methyl-5-nitrocatechol		[ng m^{-3}]	0.140	0.236	0.248	0.022	3	0.381	0.334	0.165	12
	3-methyl-5-nitrocatechol		[ng m^{-3}]	0.070	0.355	0.292	0.122	3	0.523	0.581	0.245	13
	3methyl4nitrocatechol		[ng m^{-3}]	0.124	0.195	0.195		1	0.925	0.281	1.096	7

Table S3. Species analyzed from fuel samples collected at La Paz and El Alto

	Sample#	***Al***	***Cr***	***Mn***	***Fe***	***Co***	***Ni***	***Cu***	***Zn***	***As***	***Ag***	***Cd***	***Pb***
		mg/l	mg/l	mg/l	mg/l	mg/l	mg/l	mg/l	mg/l	mg/l	mg/l	mg/l	mg/l
gasoline	1	13.7	3.96	63.0	2.81	0.05	0.23	0	0.85	4.00	0.12	0.002	0.10
gasoline	2	8.23	3.84	67.3	0.00	0.03	0.10	0	1.68	3.47	0.09	0.003	0.10
gasoline	3	8.54	3.51	61.7	0.00	0.03	0.07	0	1.71	3.07	0.01	0.004	0.10
diesel	4	14.9	9.82	0.66	0.00	0.02	0.13	0	7.85	4.00	0.01	0.005	0.25
diesel	5	15.8	8.81	0.41	0.00	0.02	0.13	0	6.55	3.74	0.00	0.007	0.27
diesel	6	35.0	10.2	0.91	11.6	0.02	0.11	0	7.49	4.36	0.01	0.011	0.28

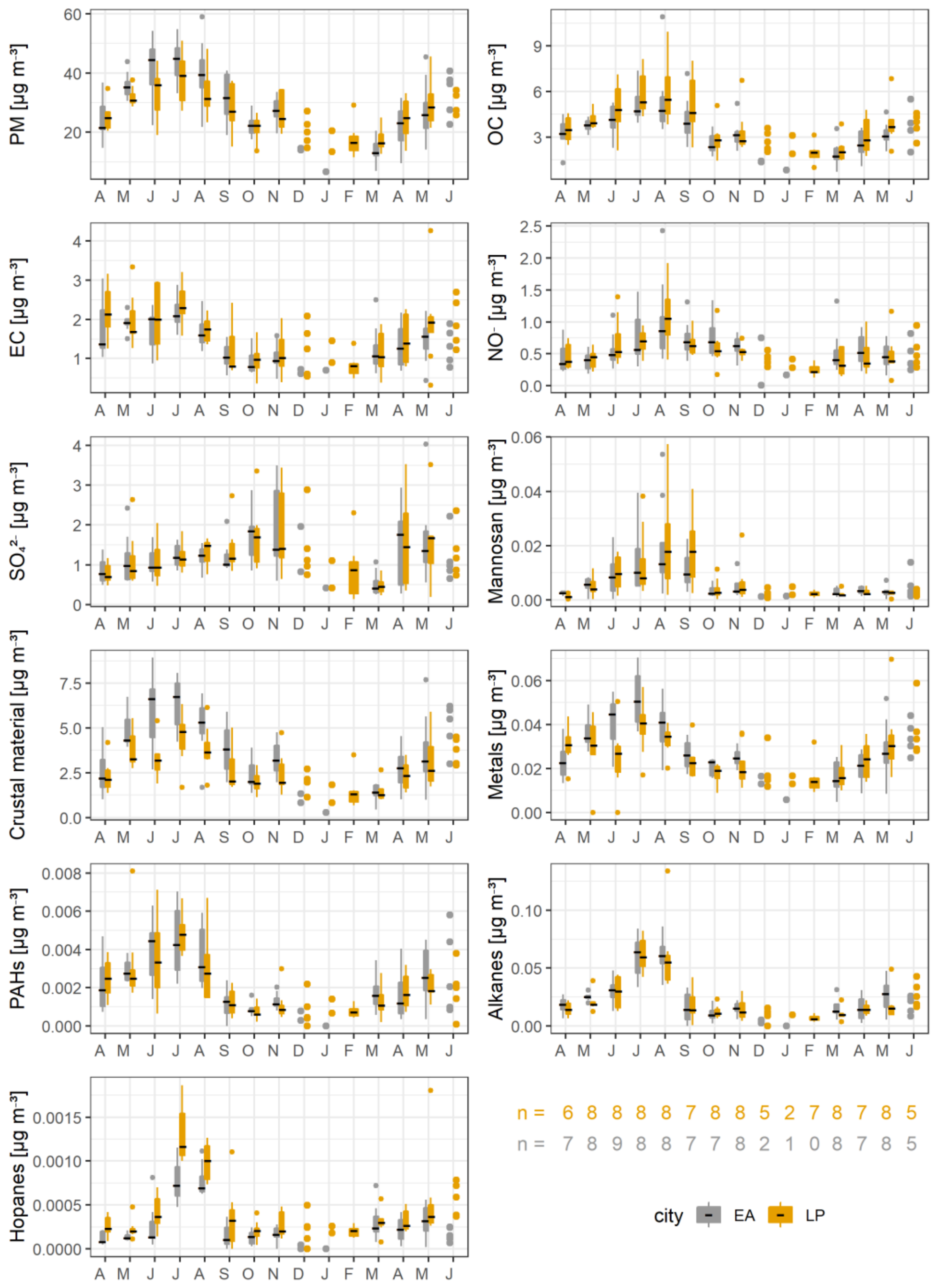

Figure S3. Monthly variation of major contributor species to PM_{10}, crustal material comprises: Al, Fe, Ti, Ca, Mg, K, Mn, P; metals comprises: Co, Ni, Cu, Zn, As, Rb, Sr, Cd, Sn, Sb, Pb; PAHs is the sum of: Phe, An, Fla, Pyr, Tri, Ret, BaA, Chr, BeP, BbF, BkF, BaP, BghiP, DBahA, IP, Cor; alkanes are the sum of C20-C31, hopanes the sum of HP3 and HP4; and n is the number of filters collected in the corresponding month at each site.

Figure S4. Chemical profile of single-site sources of PM_{10}

El Alto La Paz

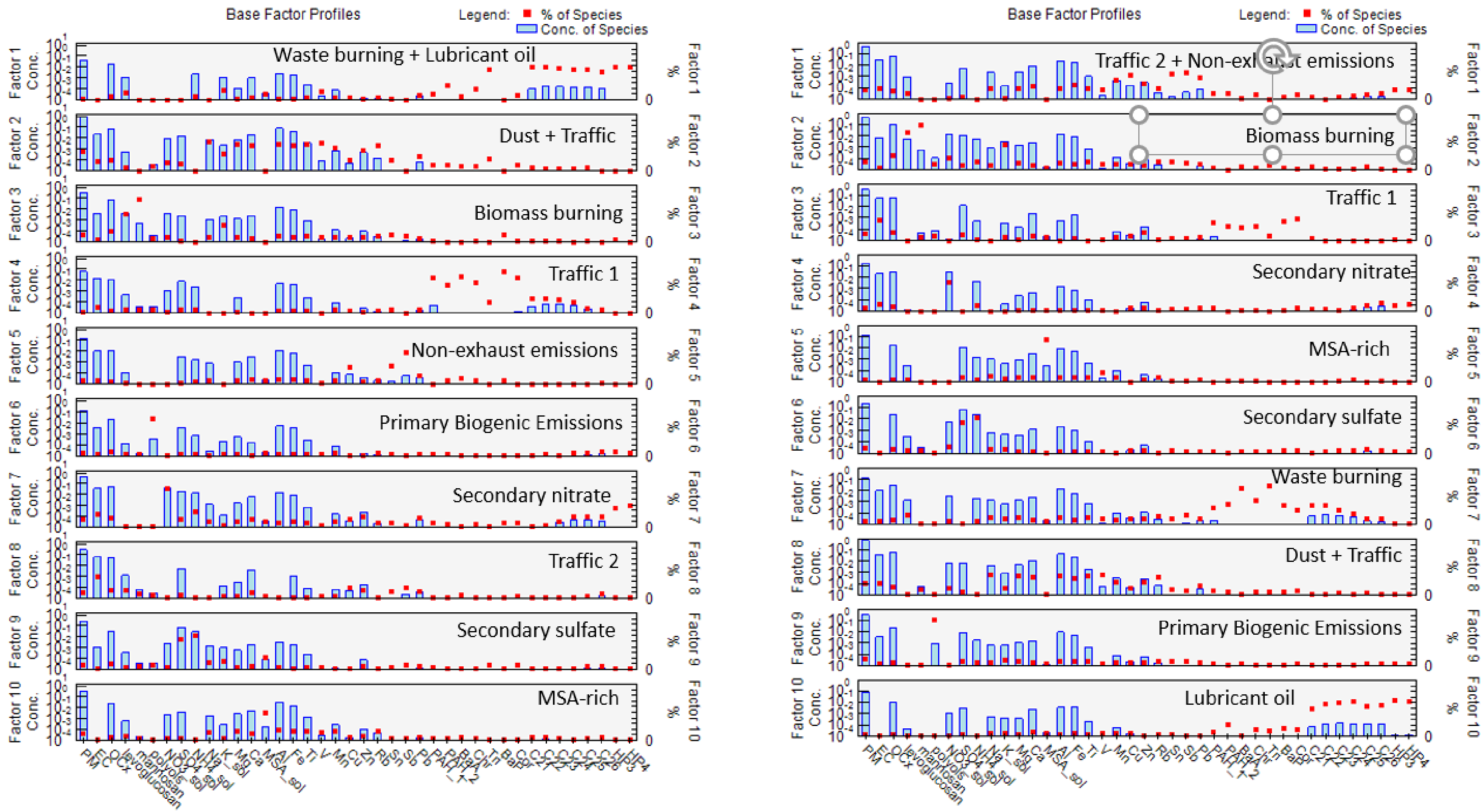

Figure S5. Percentage contribution of sources to total ambient PM (single site approach)

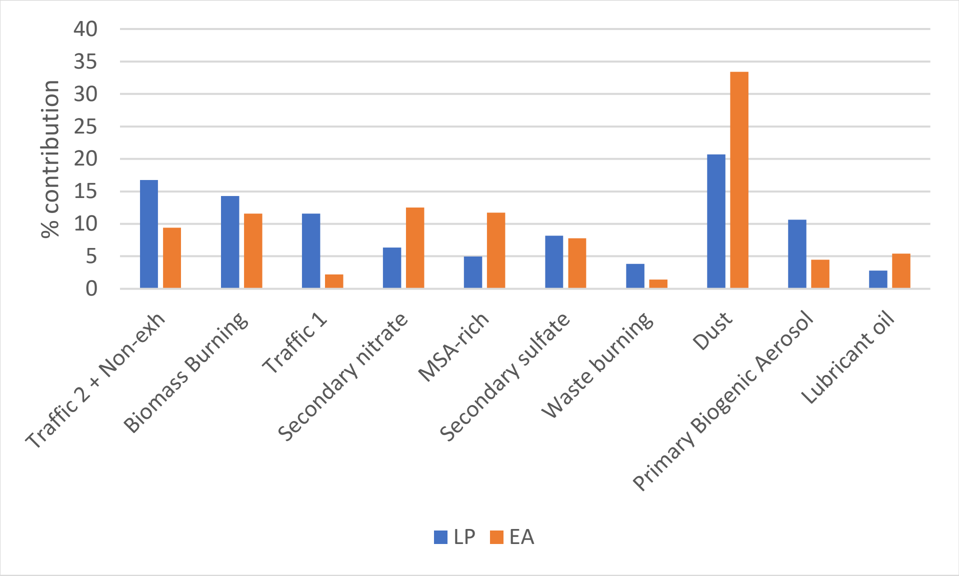

Table S4. Bootstrap mapping of single site solution El Alto

	Waste burning + Lubricant oil	Dust	Biomass burning	Traffic 1	Non-exhaust emissions	Primary Biogenic Aerosols	Secondary nitrate	Traffic 2	Secondary sulfate	MSA-rich	Unmapped
Boot Factor 1	98	0	0	2	0	0	0	0	0	0	0
Boot Factor 2	0	100	0	0	0	0	0	0	0	0	0
Boot Factor 3	0	0	100	0	0	0	0	0	0	0	0
Boot Factor 4	5	0	0	95	0	0	0	0	0	0	0
Boot Factor 5	0	0	0	0	98	1	0	0	1	0	0
Boot Factor 6	2	0	0	0	0	98	0	0	0	0	0
Boot Factor 7	0	0	0	0	0	0	100	0	0	0	0
Boot Factor 8	20	3	0	8	2	0	5	61	1	0	0
Boot Factor 9	0	0	0	0	0	0	0	0	100	0	0
Boot Factor 10	0	0	0	0	0	0	0	0	0	100	0

Table S5. Bootstrap mapping of single site solution La Paz

	Traffic 2 + Non-exhaust	Biomass Burning	Traffic 1	Secondary nitrate	MSA-rich	Secondary sulfate	Waste burning	Dust	Primary Biogenic Aerosols	Lubricant oil	Unmapped
Boot Factor 1	84	1	3	1	1	0	4	3	0	3	0
Boot Factor 2	0	100	0	0	0	0	0	0	0	0	0
Boot Factor 3	11	0	80	0	0	1	5	1	0	2	0
Boot Factor 4	0	0	0	99	0	0	0	0	0	1	0
Boot Factor 5	0	0	0	0	100	0	0	0	0	0	0
Boot Factor 6	0	0	0	0	0	100	0	0	0	0	0
Boot Factor 7	2	0	2	0	0	0	94	1	0	1	0
Boot Factor 8	0	0	0	0	0	0	1	98	0	1	0
Boot Factor 9	0	0	0	0	0	0	0	0	100	0	0
Boot Factor 10	3	0	1	0	0	0	3	1	0	92	0

Table S6. Spearman correlations between chloride and each of the resolved sources of PM. Strongest correlations are found between Cl- and Waste burning, secondly with TR1 and Non-exhaust.

		Waste burning	Sec. sulfate	TR1	MSA-rich	Lubricant	BB	Dust	Sec. Nitrate	Non-Exhaust	PBA	TR2
Spearman	Cl- EA	0.75	-0.22	0.57	0.34	0.28	0.47	0.59	-0.24	0.67	-0.19	0.25
	Cl- LP	0.67	0.01	0.61	0.39	0.49	0.53	0.45	0.19	0.57	-0.25	0.44

Test of Similarity of Chemical Profiles

In source apportionment studies, factors are labeled according to their chemical profile and its similarity to what was previously reported in the literature. Although the source identification is based on the specific tracers of the different sources, the exact chemical profile of sources with the same name could vary from site to site. Thus, a metric to quantitively evaluate the similarity between two factors was proposed by Belis et al. 2015 and Pernigotti & Belis, 2018. Two parameters are considered to establish given similarity: the Pearson distance (PD) and the similarity Identity distance (SID), defined as follows:

$$PD = 1 - r^2 \quad [S1]$$

$$SID = \frac{\sqrt{2}}{m}\sum_{j=1}^{m}\frac{|x_j - y_j|}{x_j + y_j} \quad [S2]$$

Where m is the number of common species existing between the two compared profiles and, x and y are the relative mass of the species j in each factor profile. According to Pernigotti & Belis, 2018, PD < 0.4 and SID < 1 are considered as acceptable criteria for profile similarity.

This method was used to evaluate the similarity of the resolved factors in La Paz-El Alto with what was found in France by Borlaza et al., 2021 and Weber et al., 2019 (Figure S6). From the 11 resolved sources, only 8 were comparable with was obtained from the French-sites source apportionment, out of which 4 resulted to be significantly similar to what was observed in France: primary biogenic aerosols, biomass burning, secondary sulfate and traffic 2. Although waste burning was not among the identified sources in France, this factor was compared to the industrial emissions observed in France. The disparities between the remaining factors (dust, secondary nitrate, MSA-rich and traffic 1) was largest in the PD parameter, which is highly sensitive to variation in the major mass fractions of the PM, and will be discussed below.

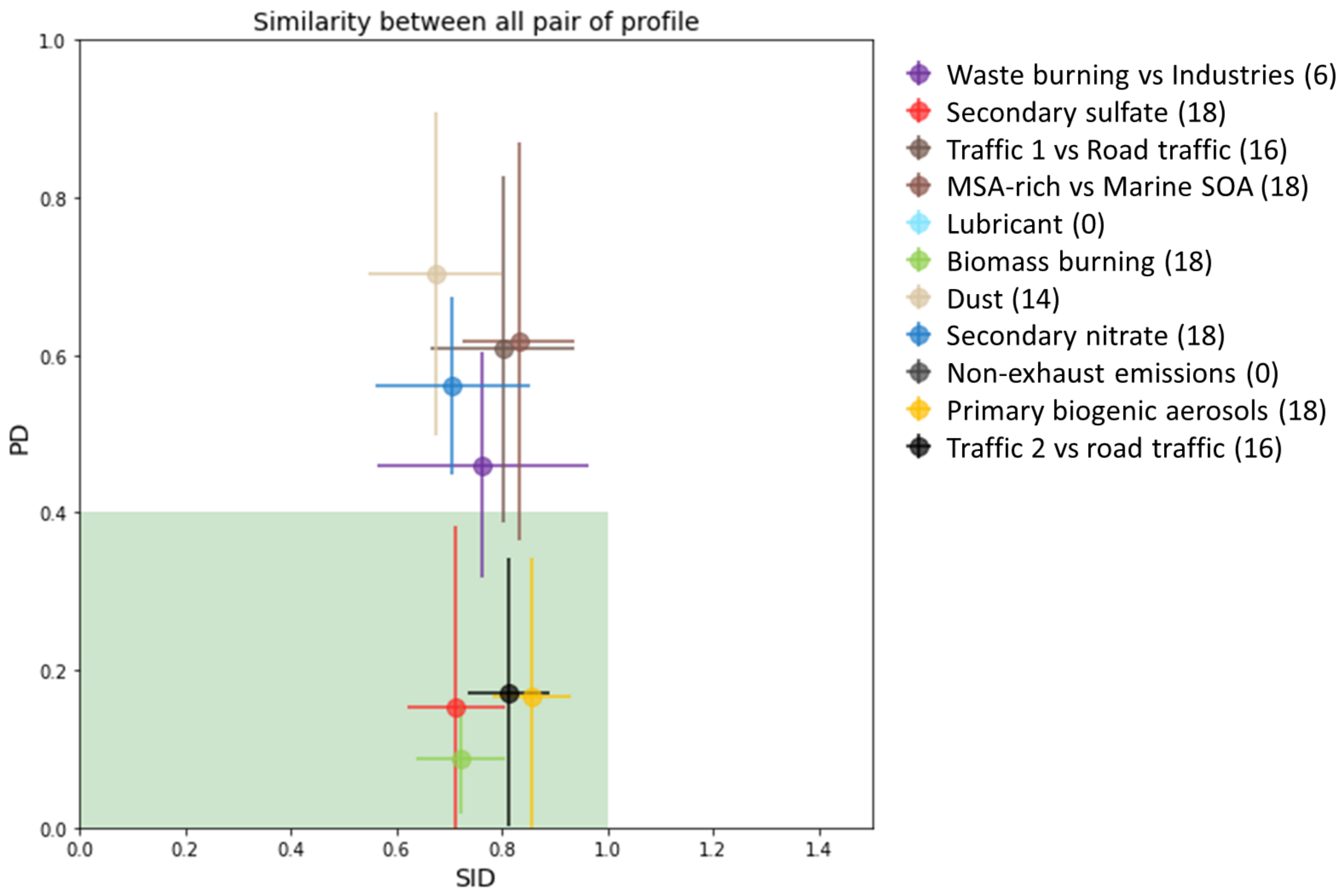

Figure S6. Similarity plot of the sources of PM_{10} in La Paz-El Alto and the sources identified by Borlaza et al. 2021 and Weber et al. 2019, by pairs, of profiles belonging to the same factor/source category. The mean ± standard deviation (sd) for each source category are plotted (circles correspond to the mean and lines to the sd on both axis). The green box highlights the acceptable area for profile similarity according to Pernigotti & Belis, 2018.

It was observed that the largest difference between the dust profiles, was the relative abundance of EC, OC, sulfate and nitrate assigned to the factors. The abundance of such species in the dust profiles in France was considerably higher compared to La Paz. In contrast, the relative concentrations of Al and Fe were generally higher for LP-EA. This shows that not only the composition of dust but the aging of the air masses carrying it are different. Similarly, for secondary nitrate, the OC and EC relative concentrations found in the secondary nitrate factor in LP-EA was generally higher than in France. This is likely because the main source of secondary-nitrate precursors in LP-EA are vehicular gaseous emissions and since the process through which secondary nitrate is formed is a relatively fast chemical process, the PMF was not able to fully separate both factors. On the other hand, nitrate relative concentrations were 2 to 4 times higher than what was observed in LP_EA. The largest difference observed in the MSA-rich chemical profiles, that led to high PD values, were the relative abundances of OC, sulfate, Al and Fe. Specifically, OC and sulfate where repeatedly higher in France, which gives an idea of the aging processes that secondary marine organic aerosols undergo. In contrast, in LP-EA, Al and Fe relative masses were significantly higher than in France. This is likely due to the mixing that takes place during the transport of this secondary aerosols across the Altiplano until reaching the metropolis. Traffic 1 had noticeably higher concentrations of Al and Fe in LP-EA but lower OC, sulfates and nitrates. In contrast, high OC relative concentrations in traffic 2, primary biogenic emissions, secondary sulfate and biomass burning, in both LP-EA and France pull the PD towards lower values.

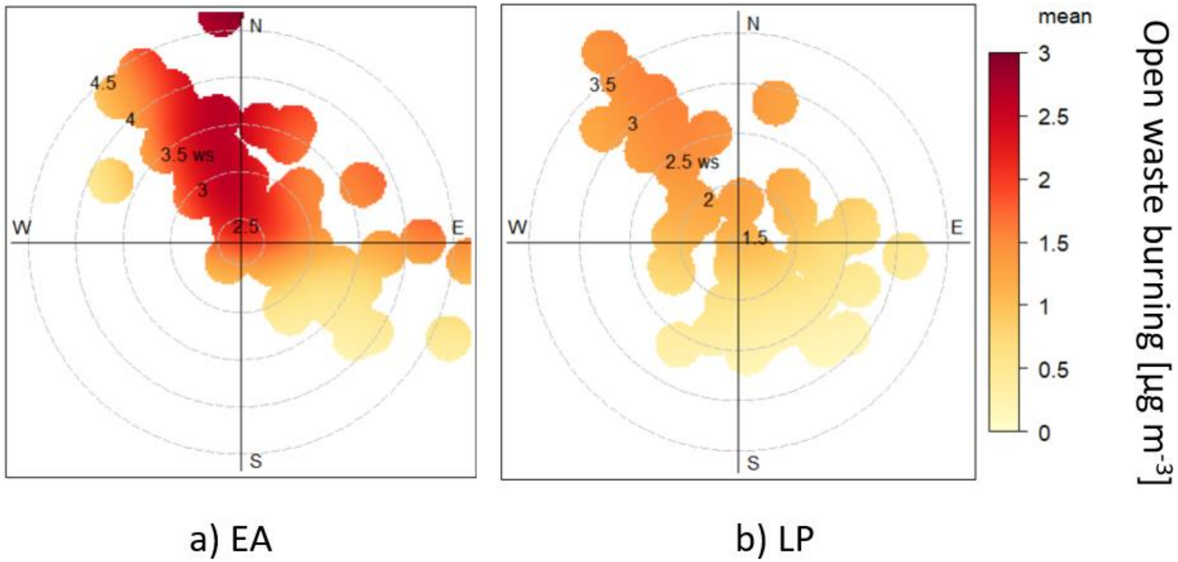

Figure S7. Polar plot showing the mean concentrations attributed to open waste burning and the associated wind speed (m s^{-1}) and wind direction.

References

Belis, C. A., Pernigotti, D., Karagulian, F., Pirovano, G., Larsen, B. R., Gerboles, M., and Hopke, P. K.: A new methodology to assess the performance and uncertainty of source apportionment models in intercomparison exercises, Atmos. Environ., 119, 35–44, https://doi.org/10.1016/j.atmosenv.2015.08.002, 2015.

Besombes, J. L., Maître, A., Patissier, O., Marchand, N., Chevron, N., Stoklov, M., and Masclet, P.: Particulate PAHs observed in the surrounding of a municipal incinerator, Atmos. Environ., 35, 6093–6104, https://doi.org/10.1016/S1352-2310(01)00399-5, 2001.

Borlaza, L. J. S., Weber, S., Uzu, G., Jacob, V., Cañete, T., Micallef, S., Trébuchon, C., Slama, R., Favez, O., and Jaffrezo, J. L.: Disparities in particulate matter (PM_{10}) origins and oxidative potential at a city scale (Grenoble, France) - Part 1: Source apportionment at three neighbouring sites, Atmos. Chem. Phys., 21, 5415–5437, https://doi.org/10.5194/acp-21-5415-2021, 2021.

Cavalli, F., Viana, M., Yttri, K. E., Genberg, J., and Putaud, J. P.: Toward a standardized thermal-optical protocol for measuring atmospheric organic and elemental carbon:

The eusaar protocol, Atmos. Meas. Tech., 3, 79–89, 2010.

Golly, B.: Etude des sources et de la dynamique atmosphérique de polluants organiques particulaires en vallées alpines : apport de nouveaux traceurs organiques aux modèles récepteurs, 292, 2014.

Jaffrezo, J. L., Aymoz, G., and Cozic, J.: Size distribution of EC and OC in the aerosol of Alpine valleys during summer and winter, Atmos. Chem. Phys., 5, 2915–2925, https://doi.org/10.5194/acp-5-2915-2005, 2005.

Pernigotti, D. and Belis, C. A.: DeltaSA tool for source apportionment benchmarking, description and sensitivity analysis, Atmos. Environ., 180, 138–148, https://doi.org/10.1016/j.atmosenv.2018.02.046, 2018.

Piot, C., Jaffrezo, J. L., Cozic, J., Pissot, N., El Haddad, I., Marchand, N., and Besombes, J. L.: Quantification of levoglucosan and its isomers by High Performance Liquid Chromatography-Electrospray Ionization tandem Mass Spectrometry and its applications to atmospheric and soil samples, Atmos. Meas. Tech., 5, 141–148, https://doi.org/10.5194/amt-5-141-2012, 2012.

Querol, X., Alastuey, A., Rodriguez, S., Plana, F., Mantilla, E., and Ruiz, C. R.: Monitoring of PM10 and PM2.5 around primary particulate anthropogenic emission sources, Atmos. Environ., 35, 845–858, https://doi.org/10.1016/S1352-2310(00)00387-3, 2001.

Weber, S., Salameh, D., Albinet, A., Alleman, L. Y., Waked, A., Besombes, J. L., Jacob, V., Guillaud, G., Meshbah, B., Rocq, B., Hulin, A., Dominik-Sègue, M., Chrétien, E., Jaffrezo, J. L., and Favez, O.: Comparison of PM10 sources profiles at 15 french sites using a harmonized constrained positive matrix factorization approach, Atmosphere (Basel)., 10, 1–22, https://doi.org/10.3390/atmos10060310, 2019.